Bioactive Materials 16 (2022) 173–186

Contents lists available at ScienceDirect

Bioactive Materials

journal homepage: www.keaipublishing.com/en/journals/bioactive-materials

Antibiofilm and immunomodulatory resorbable nanofibrous filing for dental pulp regenerative procedures

Mauricio Gonçalves da Costa Sousa [a], Gabriela Conceição de Almeida [b], Danilo César Martins Mota [c], Rosiane Andrade da Costa [a], Simoni Campos Dias [a,e], Samuel Nunes Limberger [d], Frank Ko [f], Li Ting Lin [f], Evan F. Haney [g], Hashem Etayash [g], Beverlie Baquir [g], Michael J. Trimble [g], Ya Shen [h], Zheng Su [h], Markus Haapasalo [h], Daniel Pletzer [i], Letícia Chaves de Souza [j], Gláucia Schuindt Teixeira [j,k], Renato M. Silva [j], Robert E.W. Hancock [g], Octavio Luiz Franco [a,l], Taia Maria Berto Rezende [a,b,c,*]

[a] Post-Graduation Program in Genomic Sciences and Biotechnology, Catholic University of Brasília, Brasília, Brazil
[b] Dentistry Course, Catholic University of Brasília, Brasília, Brazil
[c] Post-Graduation Program in Health Sciences, University of Brasília, Brazil
[d] LIMA, Chemistry Institute, University of Brasília-UNB, Brasília, Brazil
[e] Animal Biology Department, Campus Darcy Ribeiro, Universidade de Brasília, Brazil
[f] Department of Materials Engineering, Faculty of Applied Science, University of British Columbia, Vancouver, Canada
[g] Department of Microbiology and Immunology, University of British Columbia, Vancouver, BC, Canada
[h] Department of Oral Biological and Medical Sciences, Faculty of Dentistry, University of British Columbia, Vancouver, Canada
[i] Department of Microbiology and Immunology, University of Otago, Dunedin, New Zealand
[j] Department of Endodontics, School of Dentistry, University of Texas Health Science Center at Houston, Houston, USA
[k] Department of Prosthesis, Faculty of Dentistry, Rio de Janeiro State University, Rio de Janeiro, Brazil
[l] Post-Graduation Program in Biotechnology, Catholic University Dom Bosco, Campo Grande, Mato Grosso do Sul, Brazil

ARTICLE INFO

Keywords:
Regenerative endodontics
Scaffolds
Nanofibers
Host defense peptides
Ciprofloxacin
IDR-1002

ABSTRACT

Multifunctional scaffolds with host defense peptides designed for regenerative endodontics are desirable nanobiotechnological tools for dentistry. Here, different scaffolds were tested for use during the pulp revascularization process, including poly(vinyl alcohol)-PVA hydrogels or resins, collagen hydrogels and poly(vinyl alcohol) PVA/Chitosan (PVA/CS) nanofibers. Based on time to degradation (21 days), nanofibers were chosen to be incorporated with ciprofloxacin and IDR-1002 (each at 50 mg/g). Nanofibers containing ciprofloxacin and IDR-1002 had anti-biofilm activity against *Enterococcus faecalis, Staphylococcus aureus* and a multispecies oral biofilm, besides anti-inflammatory activities. The *in vivo* subcutaneous tissue response to tooth fragments filled with nanofibers demonstrated a pulp-like tissue formation, when compared to empty teeth fragments. Thus, we designed a strong antimicrobial, immunomodulatory and regenerative candidate for pulp revascularization and regeneration procedures.

1. Introduction

Dental trauma can be due to acute percussive transmissions to the teeth and supporting structures, which can trigger fractures in the dental element and surrounding tissues [1]. Worldwide, about 20–30% of children under 12 have already suffered dental trauma to some degree [2]. The main etiological agents related to pulp necrosis in immature permanent teeth are trauma/injuries and dental caries [3]. Dental trauma can affect the pulp tissue, disrupting blood vessels and causing aseptic necrosis [4]. In addition, traumatized teeth can be more susceptible to the invasion of microorganisms into the pulp environment and, consequently, irreversible pulpitis and pulp necrosis [5].

Peer review under responsibility of KeAi Communications Co., Ltd.
* Corresponding author. Universidade Católica de Brasília, Pós-graduação em Ciências Genômicas e Biotecnologia, SGAN 916N – Av. W5 – Campus II – Modulo C, room C-221, Brasília-DF, Brazil.
E-mail addresses: taiambr@gmail.com, taia@p.ucb.br (T.M. Berto Rezende).

https://doi.org/10.1016/j.bioactmat.2022.01.027
Received 30 September 2021; Received in revised form 5 January 2022; Accepted 17 January 2022
Available online 1 February 2022

Irreversible pulpitis is a pro-inflammatory pulp response, involving several microorganisms that stimulate cytokines and mediators related to pulp necrosis [6]. Some well-known species such as *Enterococcus faecalis* and *Staphylococcus aureus* are found in pulp infections [7,8]. However, more than 600 species are linked to the oral biofilm, including Gram-positive and negative bacteria, and even fungi [9]. These heterogeneous microbial communities organize themselves in biofilms, and it is highly challenging to eliminate such biofilm communities the from the root canal system [10]. Furthermore, residual bacterial molecules are proposed to upregulate pro-inflammatory cytokines such as IL-1β, IL-6, and TNF-α, and induce intense inflammation and tissue necrosis [11].

The conventional endodontic treatment involves chemical and physical approaches to clean and remove most of the microorganisms, followed by filling the lost pulp space with an inert material. Nevertheless, the traditional treatment protocol becomes challenging when treating immature permanent teeth, for specific anatomical reasons [12]. Alternative approaches for treatment based on biotechnology and nanotechnology are emerging as promising options in dentistry. Regenerative endodontic therapies have been widespread in endodontics, particularly in immature permanent teeth [13]. Due to failures in cases associated with apexification therapies, recent clinical procedures have sought regenerative endodontic therapy [14]. This therapy is based on tissue engineering principles, which depend on three factors including the presence of cells, repair biomolecules and a scaffold [15]. Regarding cells, many studies have suggested that the stem cells from apical papilla (SCAPs) have an essential role in tooth regeneration and root formation [16]. Concerning repair biomolecules, the presence of growth factors and biomolecules is also of paramount importance for new tissue formation [17]. Among them, transforming growth factor-β (TGF-β) seems to be involved with fibroblast recruitment and odontogenesis [18].

Host defense peptides (HDPs) have also been reported as biomolecules that can stimulate the production of other repair mediators, as well as presenting antimicrobial and immunomodulatory activity [19]. HDPs are promising alternatives for endodontic treatment [20]. We recently demonstrated that IDR-1002 and ciprofloxacin demonstrated an *in vitro* synergistic antimicrobial effect against *S. aureus* and *E. faecalis* [21].

Another essential element for tissue engineering is the presence of a scaffold [22,23]. The ideal scaffold for pulp revascularization should be flexible and resorbable while having antimicrobial, immunomodulatory and regenerative properties [24]. In this way, many scaffolds have been developed for pulp reconstruction, including hydrogels, nanotubes, and nanofibers [22]. Nanofibers, for example, are promising scaffolds for endodontic regenerative procedures [25]. Their composition is similar to that of the extracellular matrix and this, together with their large contact surface, makes them good tissue engineering alternatives [23].

Chitosan (CS) is a linear polysaccharide composed of glucosamine and *N*-acetylglucosamine from chitin found in crustaceans, insects and the skeletal structure of crustacean-associated bacteria or fungi [26]. Due to its easy access and low cost, this polymer has been studied as an attractive source from which to create scaffolds in tissue engineering [26]. Poly(vinyl alcohol) (PVA) is another low-cost synthetic polymer with biocompatible characteristics [27]. This polymer has many applications in drug delivery and is also used in membrane preparation, polymer recycling, and food packaging [28]. PVA has been used in medicine as a scaffold for an artificial pancreas, and for hemodialysis, implantable medical devices, and drug-delivery systems [29,30]. The PVA and CS combination has shown several advantages such as improving their biochemical properties and time to degradation [31].

Here, we aimed to produce an appropriate scaffold for the drug-delivery of ciprofloxacin and IDR-1002 for pulp regenerative procedures. Initially, we produced different scaffolds, including PVA hydrogel, PVA resin, collagen hydrogel and PVA, CS, or PVA/CS nanofibers. Based on scaffold degradation properties, we chose PVA/CS nanofibers to incorporate ciprofloxacin, IDR-1002 or both. Moreover, we also characterized these scaffolds and evaluated their biological activities *in vitro* and *in vivo* (Fig. 1). Our data suggest the design of a multifunctional nanofibrous scaffold for regenerative endodontic procedures.

2. Materials and methods

2.1. Different candidate scaffolds

PVA (Dinâmica, São Paulo, Brazil) hydrogels were prepared by the freezing-thawing method [32] (supplementary material). PVA resins were obtained from PVA hydrogels prepared by the freezing-thawing method [32]. Collagen (Gibco, Life technologies, Carlsbad, USA) hydrogels were polymerized by the chemical method (supplementary material) [33]. Regarding nanofiber production, distinct concentrations of PVA and chitosan (CS) (low molecular weight, Sigma Aldrich, St. Louis, USA) or the combination of both polymers were tested. PVA solutions (10%, 12.5%, and 20%) in ultrapure water, CS (10%) in a 3:1 solution of acetic acid and water, or both polymers (PVA 5% and CS 5% or PVA 7% and CS 3%) were prepared. Nanofibers were produced by electrospinning (voltage of 16 kV and a flow of 0.5 mL h^{-1}, working distance of 12 cm, NE- 2000, New Era, Pump Systems Inc.) [34].

To assess the degradation of PVA and collagen hydrogels, they were weighed and immersed in 1 mL of Dulbecco's Modified Eagle Medium (DMEM, Gibco, Life Technologies, Carlsbad, USA) supplemented with 10% fetal bovine serum (Gibco, Life Technologies, Carlsbad, USA), 5% L-glutamine (Invitrogen, Carlsbad, USA), 5% non-essential amino acids (Invitrogen, Carlsbad, USA) and 5% penicillin/streptomycin (Invitrogen, Carlsbad, USA). PVA resin discs (6 mm of diameter) were weighed (around 400 μg) and immersed in 1 mL of medium. Nanofibers (1 mg) were cut (6 mm of diameter) with a diameter paper punch and immersed in 1 mL of medium. The degradation rate was determined by discounting the initial scaffold weight, until its complete dissolution in the medium [34]. From these data, it was possible to determine the scaffold for subsequent experiments, based on the time related to pulp tissue regeneration [35]. Thus, scaffolds containing PVA nanofibers (7%) and CS (3%) that degraded in 21 days were chosen to incorporate ciprofloxacin and the immunomodulatory peptide IDR-1002.

2.2. Ciprofloxacin and IDR-1002

Ciprofloxacin was obtained from a compounding pharmacy in Brasília (Brazil) and diluted in 100% ethanol. To confirm the purity of this drug, an analysis via mass spectrometry Matrix-Assisted Laser Desorption Ionization - Time of Flight (MALDI-ToF) was performed. The purity was determined using standard European pharmacopoeia ciprofloxacin (Sigma Aldrich, St. Louis, USA) (Fig. S1). The HDP IDR-1002 was synthesized, purified (>95%), lyophilized and stored by Peptide 2.0 (Chantilly, USA) and AminoTech Research and Development (Campinas, Brazil). Before the experiments, the peptide's mass was confirmed by MALDI-ToF (Fig. S2). For the experiments, peptide IDR-1002 was quantified by weight on an ultra-sensitive scale, diluted in ultrapure water, and stored at −20 °C, until use. The peptide's stability (2.5 mg mL^{-1}) was evaluated in an acid medium (pH 2.8), containing 70% acetic acid and in extreme temperatures, between −80 and 120 °C (for 2 h) (Fig. S2 and Table S1).

2.3. Incorporation of ciprofloxacin and peptide IDR-1002 in nanofibers

The polymeric combination of PVA 7% w/v and CS 3% w/v was chosen for the experiments involving the incorporation of ciprofloxacin and IDR-1002 peptide. Thus, different concentrations (0.25%, 0.5% and 1% wt) of ciprofloxacin and IDR-1002 were tested. The polymeric solution of chitosan (3% w/v diluted in a water and acetic acid solution in the proportion of 1:3) was associated with the polymeric solution of PVA (7% w/v diluted in water) and homogenized for 5 h at 50 °C on a

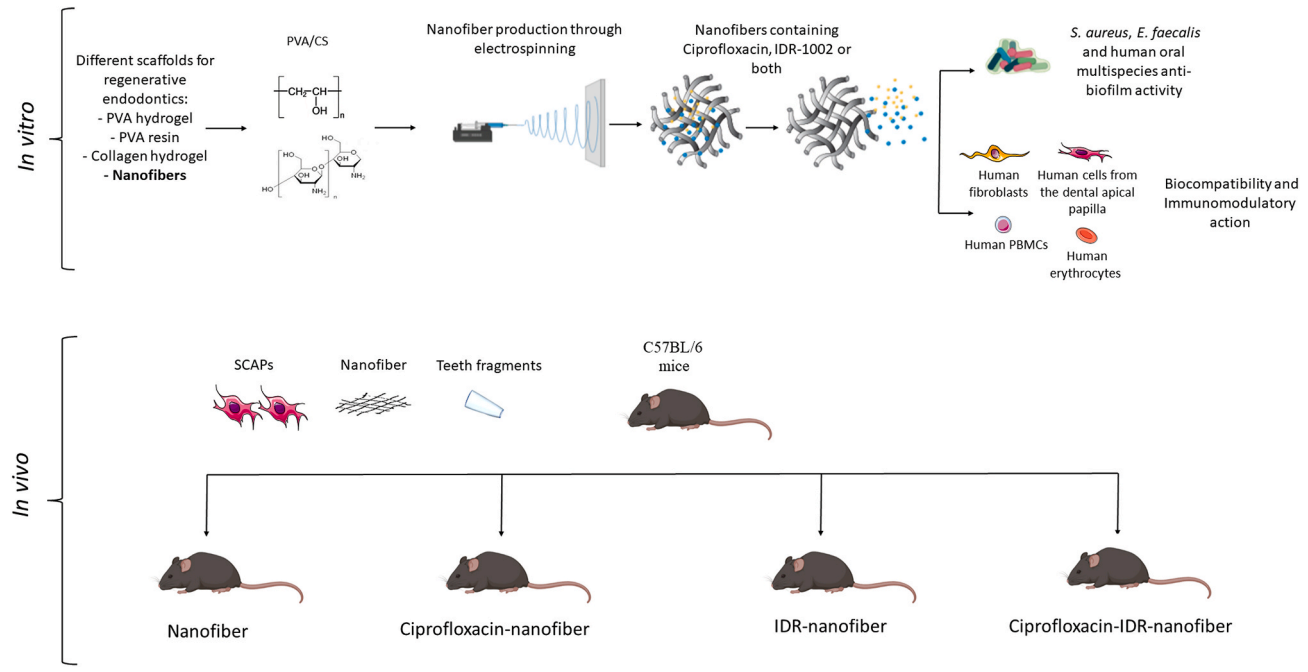

Fig. 1. Schematic workflow of the sequence of experiments developed. Initially, different scaffolds such as PVA hydrogel, PVA resin, collagen hydrogel and nanofibers were produced. Based on their degradation, nanofibers were chosen to be incorporated with ciprofloxacin and IDR-1002. The anti-biofilm, biocompatibility and immunomodulation of nanofibers were evaluated *in vitro*. Furthermore, a 3D scaffold containing nanofibers and stem cells from apical papilla were inserted on the back of C57BL/6 mice. Parts of this figure were made with Biorender.com (2020).

magnetic stirrer. After complete solubilization, ciprofloxacin, IDR-1002 or both were added to the final PVA/CS solution to be electrospun at a voltage of 16 kV and a flow of 0.5 mL h^{-1}, working distance of 12 cm (NE- 2000, New Era, Pump Systems Inc.) [34].

2.4. Antimicrobial screening of nanofibers against planktonic S. aureus and E. faecalis

The initial bacterial bioassays were performed against *E. faecalis* (ATCC 19433) and *S. aureus* (ATCC 25923). For this, 1×10^{12} CFU mL^{-1} of *E. faecalis* and 2.9×10^{8} CFU mL^{-1} *S. aureus* were used. The anti-bacterial bioassays were carried out in LB media, with 5×10^{4} CFU per well [36]. Nanofibers were cut in a circular shape (approximately 6 mm of diameter and 1 mg) and sterilized overnight in UV light. Nine experimental groups were tested: ciprofloxacin (1%, 0.5% and 0.25% wt), IDR-1002 (1%, 0.5% and 0.25% wt), and ciprofloxacin together with IDR-1002 (1% wt, 0.5% wt, and 0.25% wt of each). This experiment was performed in 96-well culture plates incubated at 37 °C for 24 h, 48 h, 72 h, and 7 days. After each experimental time, 1 μL of each group was collected and inoculated in Petri dishes with LB agar medium and incubated again at 37 °C. After 24 h, the number of CFUs was counted and compared to the control groups. Based on the bactericidal activity, nanofibers containing 0.5% of ciprofloxacin, 0.5% of IDR-1002 and 0.5% of both molecules were selected for further experiments.

2.5. Characterization of CIP-IDR-1002 loaded nanofibers

The morphological characteristics and diameter of nanofibers were evaluated by scanning electron microscopy (SEM, Fesem, ULTRA 55, Zeiss, Oberkochen, Germany). Nanofibers were fixed using double-sided carbon conductive tape and sputter-coated with a thin layer of gold (20 nm) using the Sputter Coat Emitech K550 prior to SEM analysis. The generated images were captured, and the nanofiber's diameter and pore area were determined using the Image J Tool for Windows, version 3.0. Furthermore, to determine the presence of ciprofloxacin and IDR-1002, nanofibers were incubated for 24 hours in ultrapure water and 37 °C. The presence of both molecules in the eluent was detected by high-performance liquid chromatography (C18 Shimadzu column with an injection rate of 0.6 mL min^{-1} in an isocratic method with 20% acetonitrile). The presence of both molecules was determined by a standard curve of ciprofloxacin 20 μg mL^{-1} and IDR-1002 20 μg mL^{-1}. Besides, to confirm the mass of both molecules, fractions compatible with the retention time of ciprofloxacin and IDR-1002 were collected and evaluated by MALDI-ToF. The monoisotopic mass was obtained from mass spectrometry (Bruker Daltonics, Billerica, USA), using the reflected and positive operating method of 100 and 1200 Da, with external calibration. To determine and characterize the presence of ciprofloxacin and IDR-1002 on the fibers, Fourier Transform Infrared Spectrometry (FTIR, Thermo-Nicolet 6700P FTIR Spectrometer, USA) was also performed. Nanofibers (6 mm in diameter, 1 mg) were conducted in the acoustic mode in the frequency range 4000–400 cm^{-1} with more than 250 consecutive scans and a resolution of 8 cm^{-1}.

2.6. Ciprofloxacin and IDR-1002 release profile, degradation and swelling

The *in vitro* release profile of both ciprofloxacin and IDR-1002 were evaluated through the elution method [37]. Nanofibers (6 mm of diameter and 1 mg) were cut and immersed in 2 mL Eppendorf tubes with 400 μL of water or PBS solution. The tubes were incubated at 37 °C for 24, 48, 72 h, 7 days, 14 days, and 21 days. At the mentioned time intervals, 50 μL from all solutions was taken and analyzed using HPLC. The evaluation of nanofibers swelling and degradation from experimental groups that followed for the subsequent experiments was carried out to determine their stability in aqueous medium [34]. Nanofibers (6 mm, 1 mg) were stored with PBS (1 mL) and incubated at 37 °C in the experimental periods of 24 h, 48 h, 72 h, 7 days, 14 days and 21 days. The initial weight (IW) of the untreated nanofibers was used to calculate the degree of swelling and degradation, as shown in the formula: % of swelling = [(IW–FW)/FW] x 100; % weight remaining = (FW–IW) x 100, where IW = initial weight and WF = final weight.

2.7. Anti-biofilm activity of nanofibers against E. faecalis and S. aureus

Nanofibers containing 0.5% ciprofloxacin, 0.5% IDR-1002 and the combination of both were tested against the *E. faecalis* (VP3-181) and *S. aureus* (ATCC 25923) biofilms on hydroxyapatite discs (7.6 mm in diameter and 0.6 mm in thickness, Clarkson Chromatography Products, South Williamsport, USA) [38,39]. Bacteria were pre-inoculated from a colony in 5 mL of Brain Heart Infusion BHI medium (for *E. faecalis*) and tryptic soy broth TSB supplemented with 1% glucose (for *S. aureus*). Twenty-four h later, bacteria (1 mL, 0.1 OD) were seeded on the hydroxyapatite discs in a 24-well plate. The plates were then incubated under anaerobic conditions at 37 °C, for 7 days (*E. faecalis*) and under aerobic conditions for 2 days (*S. aureus*). After biofilm growth on the hydroxyapatite discs, nanofibers (6 mm in diameter and 1 mg) incorporated or not with ciprofloxacin, IDR-1002 or both were gently placed on the biofilms. All groups were treated with triphenyl tetrazolium chloride (TTC, Sigma Aldrich) (0.05% per well) to determine the cell viability of treated biofilms.

2.8. Anti-biofilm activity of nanofibers against human multispecies oral biofilm

Ciprofloxacin-nanofibers, IDR-nanofibers and ciprofloxacin-IDR-nanofibers were tested against human multispecies oral biofilm [40]. For this purpose, supragingival and subgingival plaques were collected from 2 adult volunteers (approved by the British Columbia University ethics committee - H12-02430) and suspended in brain heart infusion broth (BHI MD, Becton Dickinson, USA). Separate lots of biofilms from each donor were grown. HA discs coated with bovine skin collagen (Sigma Aldrich) were placed in a 24-well plate containing 1.80 mL of BHI and plate suspension (0.2 mL per well) and incubated in anaerobic conditions at 37 °C. After seven days for biofilm formation, a new medium was added (350 μL per well) and discs were treated with ciprofloxacin-nanofibers, IDR-nanofibers, or ciprofloxacin-IDR-nanofibers. Plates were incubated again under anaerobic conditions at 37 °C, for 24 h. Samples for confocal laser microscopy involved the use of 2 discs from each donor. Biofilm discs were washed with PBS for 1 min to remove the culture medium. They were then stained with SYTO 9 and propidium iodide (live/dead Backlight Kit; Thermo Fisher Scientific, Carlsbad, USA). The presence of dead (red) and living (green) cells was evaluated at 100× magnification in 5 different regions of the disc, and the three-dimensional volume images were constructed with the Imaris 7.2 software (Bitplane Inc).

2.9. Nanofiber in vitro biocompatibility

The direct contact of nanofibers with different cells present in the endodontic regenerative environment was performed by fixing nanofibers on 96 well plates with porcine gelatin (1.5%) (Sigma Aldrich) (supplementary material). Nanofiber biocompatibility was performed against different human cells, such as human fibroblasts (Hfib), cells from the human dental papilla, human peripheral blood mononuclear cells (PBMCs) and human erythrocytes. All these experiments were approved by the human ethics committee (University of British Columbia and Catholic University of Brasília). Hifb and human cells were incubated with supplemented DMEM medium, and PBMCs were incubated with supplemented Roswell Park Memorial Institute RPMI medium (Supplementary material). In accordance with the parameters of ISO 10933–5, 1×10^4 cells (for Hfib and cells from apical papilla) and 1×10^5 cells per well were used [41]. The MTT assay was used to evaluate cell viability of Hfib and cells from apical papilla [42]. A total of 1×10^5 PBMCs were used to test the nanofiber's cytotoxicity. A cytotoxicity assay on PBMC cells was performed by measuring the release of the enzyme lactate dehydrogenase LDH after 24 h of incubation [43]. The hemolytic assay was performed on human erythrocytes (supplementary material). We compared the data with free ciprofloxacin, IDR-1002, or both molecules to confirm the biocompatibility profile of nanoformulations.

2.10. Nanofiber in vitro immunomodulatory profile

Nanofibers were fixed to the bottom of the 96-well plates with porcine gelatin, as previously described, to guarantee their direct contact with human immune cells (PBMCs). After 24 h of incubation, the supernatant of the stimulated cultures was collected and stored at - 80 °C until the day of the experiment. As endodontic infection processes are polymicrobial, PBMCs were stimulated with LPS (*Pseudomonas aeruginosa*, Sigma Aldrich) and LTA (*S. aureus*, Sigma Aldrich, St. Louis, USA), mimicking an *in vitro* infection. Cytokines involved with the pro-inflammatory activity (IL-1β, IL-6 and TNF-α) or anti-inflammatory activity and tissue repair (IL-10 and TGF-β) were measured by Enzyme-linked immunosorbent assay (ELISA, eBiosciences and Invitrogen, Thermo Fisher). We compared the data with free ciprofloxacin, IDR-1002, or both molecules to confirm the immunomodulatory profile of nanoformulations.

2.11. 3D cell culture model with SCAPs and nanofiber-cell interaction

Teeth indicated for extraction for orthodontic reasons were obtained from the School of Dentistry, University of Texas Health Sciences Center at Houston. This study was approved by the human and animal ethics committee (194826). Uniradicular fragments were examined and disinfected with 6% sodium hypochlorite and kept in 1.5% sodium hypochlorite until use. Dental fragments were cut and standardized at 5 mm in length. A 1.5 mm root canal diameter was obtained by using a 1014 diamond bur. One portion of the tooth was sealed with mineral trioxide aggregate MTA (Dentsply, Tulsa, USA) and the other part was left open. The dental fragments were treated with EDTA 17% (Dentsply, Tulsa. USA) before use and filled with prefabricated nanofibers. Nanofibers were cut (3 mm wide x 5 mm high), manually modeled on a 3D structure and inserted into the dental fragments. Dental fragments were fixed to the 24-well plates using 1.5 mL of 20% bovine porcine gelatin (Sigma Aldrich, St. Louis, USA). RP89 stem cells from apical papilla (SCAP) were cultured in α-MEM (Gibco, Life Technologies, Carlsbad, USA) medium, containing 10% fetal bovine serum (Gibco), 100 IU.mL^{-1} of penicillin (Invitrogen), 100 μg mL^{-1} of streptomycin (Invitrogen), and 2 mmol L^{-1} of L-glutamine (Invitrogen). Cells were resuspended in a gelatinous medium (1.5% porcine gelatin) to construct a 3D environment involving nanofibers. Inside each artificial root canal system, 10^5 cells were used. The artificial root canal system was treated with nanofibers, ciprofloxacin-nanofibers, IDR-nanofibers, or ciprofloxacin-IDR-nanofibers. These cells were cultured in the 3D model *in vitro* with the scaffolds for 3 days and taken for the *in vivo* test. To assess the interaction between nanofibers and SCAPs, fragments containing control nanofibers and nanofibers with both ciprofloxacin and IDR-1002 were chosen for microscopy. The fragments were fixed with 2.5% glutaraldehyde and dehydrated with alcohol (from 15 to 100%). The fragments were analyzed by scanning electron microscopy (Fesem, Ultra 55, Zeiss).

2.12. Nanofiber biocompatibility in vivo

C57BL/6 female mice (5 per group, 27g and 6 weeks of age) were used for subcutaneous implantation. This project was approved by the University of Texas animal committee (194826). A sagittal incision was made in the back of mice and 2 subcutaneous pockets were created. Samples were implanted on the back of these animals, following the groups: teeth with nanofibers and SCAPs, teeth with nanofibers, teeth with nanofibers and SCAPs, teeth with ciprofloxacin-nanofibers and SCAPs; teeth with IDR-nanofibers and SCAPs and teeth with ciprofloxacin-IDR-nanofibers. Empty teeth and teeth with SCAPs were used as controls. Briefly, animals were anesthetized by isoflurane inhalation and local anesthesia (0.5% bupivacaine). A 1 cm longitudinal

incision was made on the dorsum, and, through blunt dissection, bilateral subcutaneous pockets were created in the separation of the dermis from the underlying muscle layer. The animals were kept in a cage placed on a heat pad for 2 h until they were fully recovered from the surgery, and properly positioned to allow adequate respiration as well as protect from pressure points. Mice were monitored daily after surgery for any sign of infection and inflammation. Ninety days after subcutaneous implantation, mice were euthanized by CO_2 overdose, followed by cervical dislocation. The root fragments were recovered and fixed in 10% buffered formalin at 4 °C for 24 h, followed by demineralization in 10% formic acid at 4 °C until the dentin could be cut with a blade. Samples were included in paraffin and stained with hematoxylin-eosin for microscopic analysis [44]. 5 different images were used to determine the percentage of neotissue formation and the number of inflammatory infiltrate cells per mm^2 using the software Image J Tool for Windows, version 3.0.

2.13. Statistical analysis

All experiments were carried out in technical and biological triplicates. Statistical analyses were performed by Kolmogorov-Smirnov test, followed by one-way analysis of variance (ANOVA) and Bonferroni post hoc using GraphPad Prism 6 (GraphPad Software, San Diego, CA); $p < 0.05$ was considered statistically significant.

3. Results and discussion

3.1. Nanofibers are stable scaffolds in the environment of media

Since pulp reconstruction is a complex process that requires time, the rate of degradation was evaluated as a critical factor when choosing the most suitable scaffold to be incorporated with ciprofloxacin and IDR-1002. It was observed that PVA hydrogels degraded faster (within 15 min) than other scaffolds (Fig. S3). Conversely, nanofibers made with 10% CS demonstrated higher stability in media over time, enabling maintenance for an extended period (45 days) (Fig. S3). When CS was combined with PVA in nanofibers, there was an intermediate/balanced time of degradation. Thus 5% PVA combined with 5% CS led to nanofibers that degraded in 25 days while 7% PVA/3% CS nanofibers degraded in 21 days (Fig. S3). Based on their degradation time, the latter mixed PVA/CS (7%/3%) nanofibers were chosen for incorporation of ciprofloxacin and peptide IDR-1002 for subsequent experiments. This decision was based on the potential of PVA/CS nanofibers to degrade during the time in which pulp tissue would be reconstructed [35].

3.2. Antimicrobial activity of nanofibers against planktonic bacteria was due to ciprofloxacin

PVA/CS nanofibers with different ciprofloxacin or IDR-1002 proportions were tested against planktonic *S. aureus* and *E. faecalis*. *S. aureus* is involved with pulp inflammation [45], and *E. faecalis* is a persistent microorganism found in most endodontic infections [46]. It was noticed that nanofibers incorporating 0.5% or 1% by weight ciprofloxacin had bactericidal activity against *S. aureus* and *E. faecalis* (Table 1).

Nevertheless, the lowest tested concentration of ciprofloxacin incorporated (0.25%) did not affect *S. aureus* growth and had only a bacteriostatic effect against *E. faecalis* (Table 1). In contrast, nanofibers containing just IDR-1002 did not affect the growth of either *S. aureus* or *E. faecalis* after 24 h of incubation (Table 1). The incorporation in PVA/CS nanofibers of both ciprofloxacin (0.5%) and IDR-1002 (0.5%) maintained the bactericidal ciprofloxacin activity (Table 1). Thus, the presence of IDR-1002 did not interfere with the bactericidal activity of ciprofloxacin in nanofibers at concentrations of 0.5% of each molecule. Therefore, nanofibers incorporated with ciprofloxacin and IDR-1002 0.5% were selected for the following experiments.

Table 1
Antimicrobial activity of PVA/CS nanofibers incorporated with different concentrations of ciprofloxacin, IDR-1002 or both against *S. aureus* (ATCCC 25923) and *E. faecalis* (ATCC 19433). The results were expressed according to the percent of inhibition. sd represents the standard deviation for 3 different biological triplicates and statistical significance are represented by ** ($p < 0.01$), *** ($p < 0.001$) and **** ($p < 0.0001$) compared to the control groups (ampicillin 20 μg mL^{-1} represents 100% of inhibition and only bacteria 0% of inhibition).

Nanofiber	Percent of inhibition for *S. aureus*	Antimicrobial profile for *S. aureus*	Percent of inhibition for *E. faecalis*	Antimicrobial profile for *E. faecalis*
CIP 1 % wt.	100% (sd ± 6)****	Bactericidal	100% (sd ± 4)****	Bactericidal
CIP 0.5 % wt.	**100% (sd ± 5)*****	**Bactericidal**	**100% (sd ± 6)*****	**Bactericidal**
CIP 0.25 % wt.	4% (sd ± 4)	No activity	76% (sd ± 3)****	Bacteriostatic
IDR-1002 1 % wt.	1% (sd ± 1)	No activity	3% (sd ± 2)	No activity
IDR-1002 0.5 % wt.	2% (sd ± 2)	No activity	5% (sd ± 4)	No activity
IDR-1002 0.25 % wt.	1% (sd ± 1)	No activity	1% (sd ± 1)	No activity
CIP 1% and IDR-1002 1 % wt.	100% (sd ± 3)***	Bactericidal	100% (sd ± 3)***	Bactericidal
CIP 0.5% and IDR-1002 0.5% wt.	**100% (sd ± 4)****	**Bactericidal**	**100% (sd ± 2)****	**Bactericidal**
CIP 0.25% and IDR-1002 0.25 % wt.	10% (sd ± 9)	No activity	89% (sd 5) **	Bacteriostatic

3.3. Incorporated nanofibers of ciprofloxacin and IDR-1002 showed both molecules in their composition

Based on the choice of PVA/CS nanofibers with 0.5% ciprofloxacin, IDR-1002 or both incorporated, their size, density, and pore area were determined through scanning electron microscopy (SEM). The diameter of nanofibers and their pore area are important parameters that can influence their biological activities [47]. It was observed that most of the control nanofibers had a diameter between 250 and 450 nm and pore areas between 5 and 25 μm^2 (Fig. 2a–c). Ciprofloxacin incorporation did not modify nanofiber structure (average diameter between 250 and 450 nm and pore area between 5 and 25 μm^2) (Fig. 2d–f). Interestingly, the presence of IDR-1002 modified their diameter but not their pore area (Fig. 2g–i). Thus, nanofibers incorporating IDR-1002 or ciprofloxacin plus IDR-1002 had smaller diameters (most of them between 100 and 250 nm), but similar pore area (between 5 and 50 μm^2) (Fig. 2j-l).

To confirm the presence of both ciprofloxacin and IDR-1002 on these scaffolds, they were incubated in water, and then the molecule release was determined. It was observed, by using high-performance liquid chromatography, that the retention time for ciprofloxacin, IDR-1002 or ciprofloxacin associated with IDR-1002 (8.2 min for ciprofloxacin and 14.2 min for IDR-1002) enabled the demonstration of each molecule according to the retention of standards (Fig. S4a). From these fractions, correct masses for ciprofloxacin (332.2 Da) and IDR-1002 (1652.4 Da), it was confirmed by MALDI-TOF, showing that both molecules were present on the nanofibers (Fig. S4b).

When analyzed with Fourier-transform infrared spectroscopy, PVA/CS nanofibers showed peaks at 3305 and 3535 cm^{-1}, due to O–H and

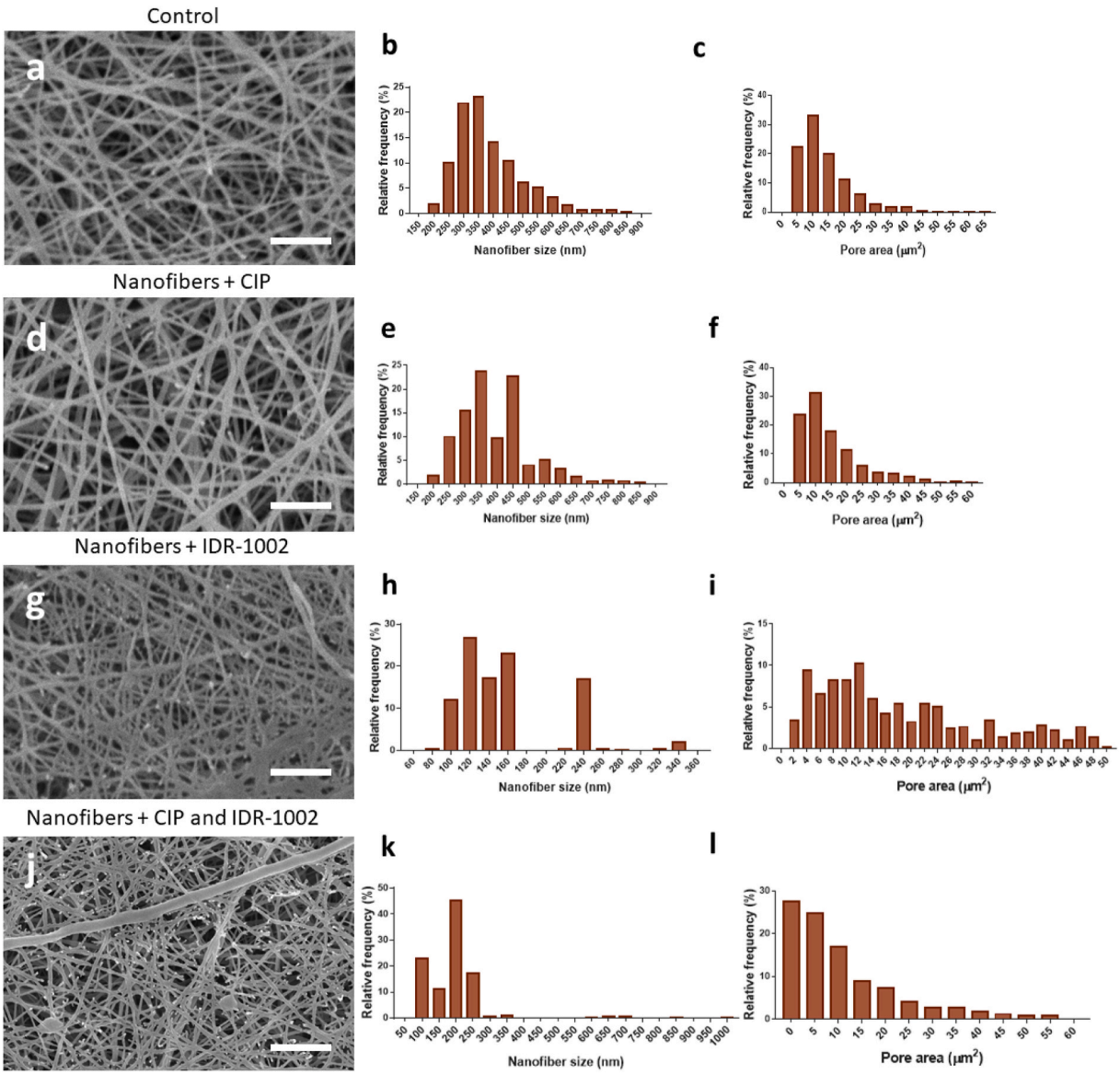

Fig. 2. SEM micrographs of nanofibers (a–c), nanofibers containing ciprofloxacin (d–f), IDR-1002 (g–i) or both (j–l) showing nanofiber morphology and porous structure. Nanofiber diameter size and nanofiber porous size distribution were calculated using Image J software 3.0. Scale bar 20 μm.

N–H stretching vibrations. Peaks at 2931 and 2910 cm^{-1} were also noted, due to asymmetric alkyl C–H stretching and symmetric alkyl C–H stretch, respectively. These peaks appeared in all samples tested and seemed wide-ranging due to overlapping frequencies of different O–H and N–H groups. Further, the characteristic peaks found around 1653 and 1556 cm^{-1} corresponded to amide I and amide II vibration bands, respectively (Fig. S5a). The peak at 1657 cm^{-1} might have arisen from the amide I band and from the ciprofloxacin quinolones. A broad peak was observed near 1085 cm^{-1}, which was due to stretching vibrations of the C–O group present in PVA/CS nanofibers, and the fluorine atom of ciprofloxacin. In the spectrum of ciprofloxacin-IDR1002-nanofibers (Fig. S5d), most of the peaks detected in Figs. S5b and S5c were observed with very intense peaks at 1728, 1646, and 1250 cm^{-1}, providing strong supporting evidence for the effective assembly of the nanofibers with both compounds.

3.4. IDR-1002 remained until nanofibers were degraded

Nanofibers generally degraded after 21 days and showed a similar swelling profile (Figs. S6a–b). In contrast, control nanofibers demonstrated a considerable swelling rate compared to all groups ($p < 0.0001$) after 14 days (weight of 6.2 mg and swelling rate of 581.25%) (Figs. S6a–b). Nanofibers incorporating both ciprofloxacin and IDR-1002 presented a higher swelling rate compared to all other nanofibers in 24 h ($p < 0.0001$), with an average weight of 1.96 mg and a percentage of 184.3% (Figs. S6a–b). On the fourteenth day, these fibers showed reduced swelling when compared to all groups ($p < 0.0001$), with an average weight of 0.6 mg and 65.6% of swelling (Figs. S6a–b). Regarding degradation, there was no significant difference between all groups over time (Figs. S6c–d). Complete degradation of nanofibers was observed on the twenty-first day of the experiment (Figs. S6c–d). Swelling is an important factor related to the biomaterial's ability to interact and absorb liquids. During pulp revascularization processes, this property might be advantageous, since it can favor bleeding control, and create a supportive microenvironment to absorb cells and growth factors [48,49]. However, high swelling might generate internal pressure on the dentin walls [50].

With regard to the ciprofloxacin and IDR-1002 release profile, the experiments were carried out both in water and in PBS. The release of antimicrobial molecules during the pulp revascularization process is

essential to ensure an aseptic environment [51]. Thus, our results showed that the release in water was faster (Fig. S7). Besides, nanofibers quickly degraded in water, which also explains their faster release in this solvent than in PBS (Fig. S7). In this sense, 99.3% of ciprofloxacin (CIP) was released from CIP-nanofibers after 1 day in water (Fig. S7a) and 84.7% in PBS (Fig. S7b), after 3 days. Regarding IDR-1002, 38.4% of this biomolecule was released after 1 day in water (Fig. S7c) from IDR-nanofibers. In contrast, only 0.5% of this peptide was released from IDR-nanofibers in PBS after 21 days (Fig. S7d). It was also shown that IDR-1002 remained on the surface while fibers were degraded. The release profile of nanofibers containing both molecules seemed like that of nanofibers containing the individual molecules. Thus, with CIP-IDR-nanofibers, both molecules were released (79.5% of ciprofloxacin and 40.2% of IDR-1002) quickly in water (Fig. S7e). In PBS, 83.7% of ciprofloxacin was released in 2 days, while IDR-1002 remained associated with the nanofiber structure, even after 21 days (0.8% of release) (Fig. S7f). These results confirm that the antimicrobial activity against planktonic cells was associated with ciprofloxacin, since although the peptide is present on nanofiber surfaces, it is not released to interact with bacteria in aqueous media. Ciprofloxacin burst release might be related to changes in the hydrogen bonding character and microstructure within the scaffold [52]. In contrast, chitosan allowed the slow and linear release of AMPs [53], which might explain low rates of IDR-1002 released from PVA/CS nanofibers.

3.5. Antibiofilm activity of the nanofibers was due to both ciprofloxacin and IDR-1002

Initially, the antibiofilm activity of nanofibers was evaluated against *S. aureus* (ATCC 25923) and *E. faecalis* (VP3-181). Biofilms are a significant challenge for endodontic therapies, since the microorganisms contained therein can trigger a pro-inflammatory process, and compromise the formation of loose connective tissue [54]. Prior to the anti-biofilm activity experiments, the scaffold inhibition zone of *S. aureus* and *E. faecalis* was determined (Fig. S8). Hydroxyapatite discs were used to mimic the dentin walls that are the main target of biofilm formation in the root canal system [55]. Thus, it was observed that after 24 h of incubation, IDR-nanofibers (72% reduction) ($p < 0.01$) and CIP-IDR-nanofibers (75% reduction) ($p < 0.01$) were able to significantly reduce metabolic cells in *S. aureus* biofilms (Fig. 3a). In contrast for *E. faecalis* biofilms, only nanofibers containing ciprofloxacin and IDR-1002 were able to reduce this biofilm (80% reduction) ($p < 0.05$, $p < 0.01$, Fig. 3b). Although IDR-1002 was minimally released from PVA/CS nanofibers, it had anti-biofilm and/or antimicrobial activity, presumably due to direct contact. Moreover, we previously demonstrated that the association of IDR-1002 with ciprofloxacin improves its antimicrobial potential [21]. The results of the anti-biofilm activity of nanostructured molecules were close to what was found with the free molecules (Fig. S9).

The impact of nanofibers on multispecies human oral biofilm was also evaluated. Human oral biofilm is composed of hundreds of microbial species, including Gram-positive and -negative bacteria as well as fungi [56]. To simulate the oral biofilm *in vitro*, we used microbes from the saliva of human volunteers and grew multispecies biofilms preformed on hydroxyapatite discs under anaerobic conditions, an experimental model that was closer to the clinical situation in the root canal system. The results analyzed by confocal microscopy also allowed better evaluation of the biofilm structures formed and killed (Fig. 4a–k). Thus, control nanofibers showed mild antibiofilm activity (18% reduction) ($p < 0.01$, Fig. 4c,h), due to the chitosan's antimicrobial properties [57]. CIP-nanofibers (60% of reduction) ($p < 0.001$) (Fig. 4d and i) and IDR-nanofibers (60% of reduction) ($p < 0.001$) (Fig. 4e and j) both significantly eradicated oral biofilm. Furthermore, nanofibers containing ciprofloxacin and IDR-1002 eradicated 78% ($p < 0.001$) of oral

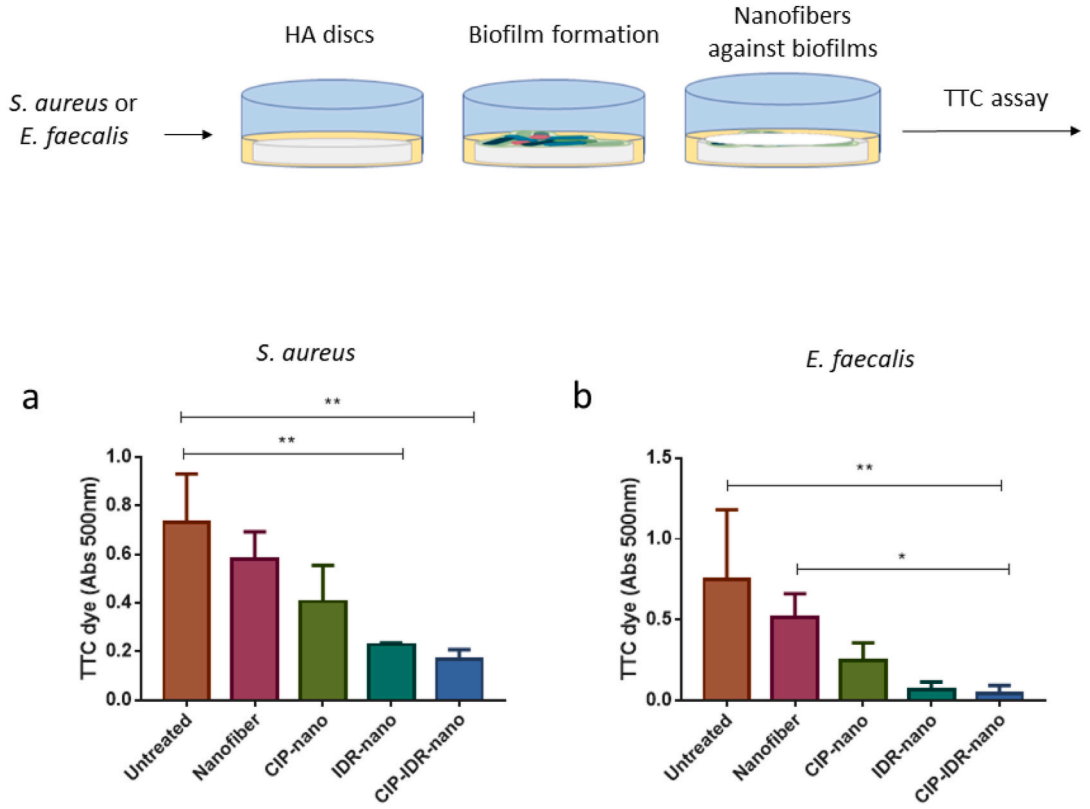

Fig. 3. Anti-biofilm activity of PVA/CS nanofibers incorporated with ciprofloxacin (CIP-nano), IDR-1002 (IDR-nano) or both (CIP-IDR-nano), against *S. aureus* (ATCC 25923) (a) and *E. faecalis* (ATCC 19433) (b) after 24 h of incubation. Bars represent the absorbance averages in 500 nm of the TTC stain. Statistical differences were represented by * $p < 0.05$ and **$p < 0.01$, after one-way ANOVA post Bonferroni test. Parts of this figure were made with Biorender.com (2020).

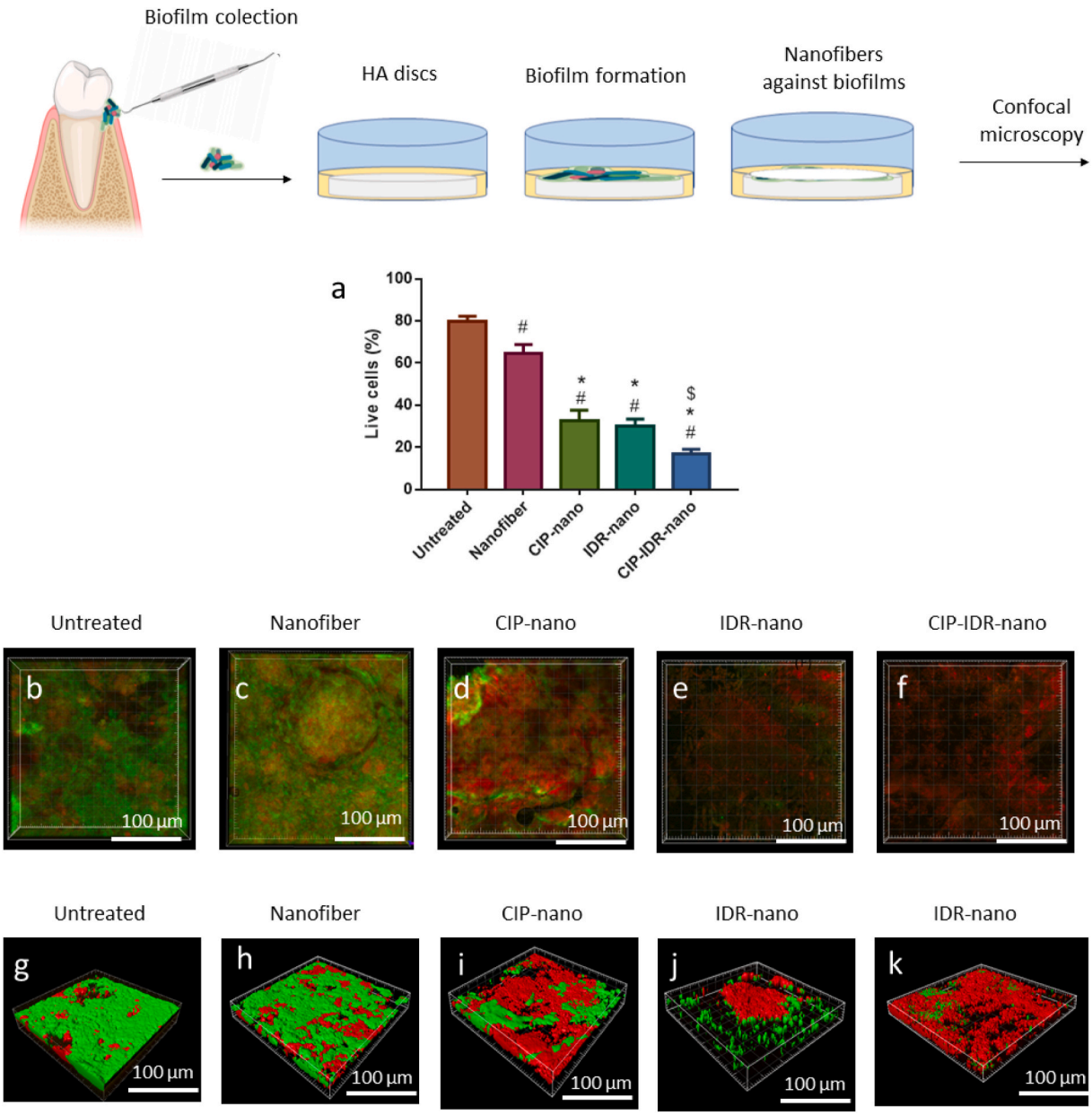

Fig. 4. Anti-biofilm activity of PVA/CS nanofibers incorporated with ciprofloxacin (CIP-nano), IDR-1002 (IDR-nano) or both (CIP-IDR-nano) against human multispecies oral biofilm. Live cells were stained with SYTO 9 (green signal), and dead cells were stained with propidium iodide (red signal). (a) represents the percentage of live cells treated with nanofibers. (b–f) represents confocal microscopy images (100 µm) after 24 h of incubation while (g–k) represents 3D biofilm constructions using Imaris 7.2. Statistical differences were represented by #$p < 0.0001$ (compared to the untreated group), *$p < 0.0001$ (compared to the nanofiber group) and \$ $p < 0.0001$ (compared to the CIP-nano and IDR-nano groups) after one-way ANOVA post Bonferroni test. Parts of this figure were made with Biorender.com (2020).

biofilm, making them the most effective biomaterials (Fig. 4f and k). The anti-biofilm activity of nanostructured molecules was close to what was found with free molecules (Fig. S10).

3.6. Nanofibers were biocompatible and presented immunomodulatory activity

The ideal biomaterial for pulp regenerative procedures should present a balance between the necessary antimicrobial activity and lack of toxicity to human cells [58]. In this regard, several cells are involved with the endodontic regenerative process and new tissue formation, including cells from the apical papilla, fibroblasts, immune cells, and erythrocytes [59]. The cytotoxic potential of direct contact with the developed nanofibers was determined against these cells. For these analyses, a cell viability assay using the metabolic dye MTT was performed in human fibroblasts and cells of the human apical papilla cultures (Fig. 5a). It was observed that none of the nanofibers significantly reduced cell viability after 24 h of incubation (Fig. 5b–c). To determine nanofiber cytotoxicity against PBMCs, LDH release was assessed. Results revealed that none of the nanofibers were toxic (Fig. 5d). Furthermore, nanofibers did not show any hemolytic potential for human erythrocytes (Fig. 5e). A critical aspect of these scaffolds is that we incorporated lower concentrations, making them more suitable for different cells. Although cellular viability and toxicity are critical aspects in determining biomaterial biocompatibility, other functions such as their impact on the immune system are key factors in selecting the best biomaterial for clinical use [60].

Regarding immunomodulatory findings, the interaction of

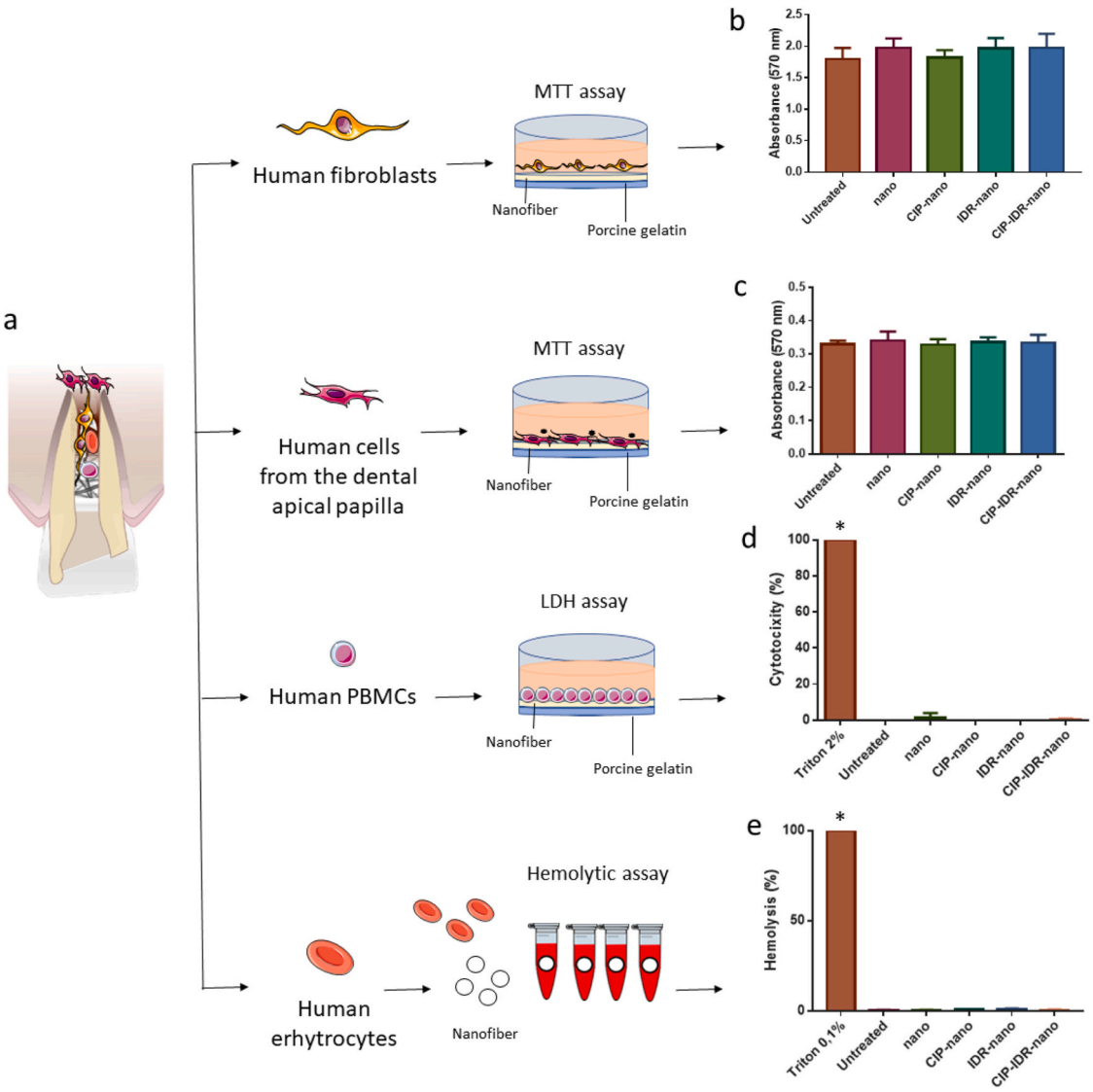

Fig. 5. Nanofiber biocompatibility. Different cells present on pulp space after pulp revascularization such as human fibroblasts, human cells from the dental apical papilla, human peripheral blood mononuclear cells, and human erythrocytes were cultivated with nanofibers (nano), nanofibers containing ciprofloxacin (CIP-nano), IDR-1002 (IDR-nano) and both (CIP-IDR-nano) (a). (b) and (c) represent the cell viability assay through MTT after 24 h of incubation. Bars represent the average of absorbances at 570 nm. (d) represents nanofiber toxicity against human peripheral blood mononuclear cells. The cytotoxic percentage (absorbance was performed at 500 nm) was obtained through LDH assay, after 24 h of incubation. (e) represents the hemolytic percentage (at 504 nm) of human erythrocytes after 1 h of incubation in direct contact with nanofibers.

biomaterials with the immune system can be an excellent weapon for tissue engineering [60]. The antigenic remnant from microorganisms that persists in the root canal system even after the use of antimicrobial substances can stimulate the production of cytokines and mediators that modulate the role of stem cell differentiation in specialized tissues, in that pro-inflammatory cytokines tend to discourage the formation of a pulp-like tissue [54]. Therefore, we mimicked an *in vitro* infection system by stimulating PBMCs with LPS (representing Gram-negative bacteria) or LTA (mimicking Gram-positive bacteria). It was observed that only CIP-IDR-nanofibers did not stimulate pro-inflammatory cytokines (IL-1β, IL-6 and TNF-α) in the absence of both LPS and LTA stimuli ($p < 0.05$, $p < 0.01$, Fig. 6a–c). Furthermore, CIP-IDR-nanofibers significantly ($p < 0.05$ or $p < 0.01$) suppressed LPS + LTA-induced pro-inflammatory cytokines (IL-1β and TNF-α almost completely suppressed, IL-6 by 64%) (Fig. 6a–c). Interestingly, IDR-nanofibers or CIP-IDR-nanofibers upregulated the anti-inflammatory cytokine IL-10 only in the presence of LPS + LTA ($p < 0.01$, Fig. 6d). Control nanofibers, IDR-nanofibers, and CIP-IDR-nanofibers all upregulated anti-inflammatory TGF-β in the presence of LPS + LTA ($p < 0.05$, $p < 0.01$, Fig. 6e). Overall, these data indicated that CIP-IDR-nanofibers had immunomodulatory activity that could favor tissue formation, especially in downregulating pro-inflammatory cytokines (IL-1β, IL-6 and TNF-α), and upregulating anti-inflammatory cytokines (IL-10 and TGF-β) in the presence of LPS + LTA (Fig. 6f). It is known that chitosan can modulate the immune system [61], possibly explaining the different profile of free ciprofloxacin and IDR-1002 when compared to the nanofiber associated ones (Fig. S11).

3.7. *Nanofibers physically interacted with SCAPs in vitro and stimulated loose connective tissue formation in vivo*

3D cell models bring *in vitro* studies closer to clinical reality [62]. For this purpose, nanofibers were modeled and shaped to adapt to root canals and cultivated *in vitro* with stem cells from apical papilla (SCAPs) and gelatin (reflecting fibrin formation during blood clotting) (Fig. 7a–d). In this experiment, control and CIP-IDR-nanofibers were

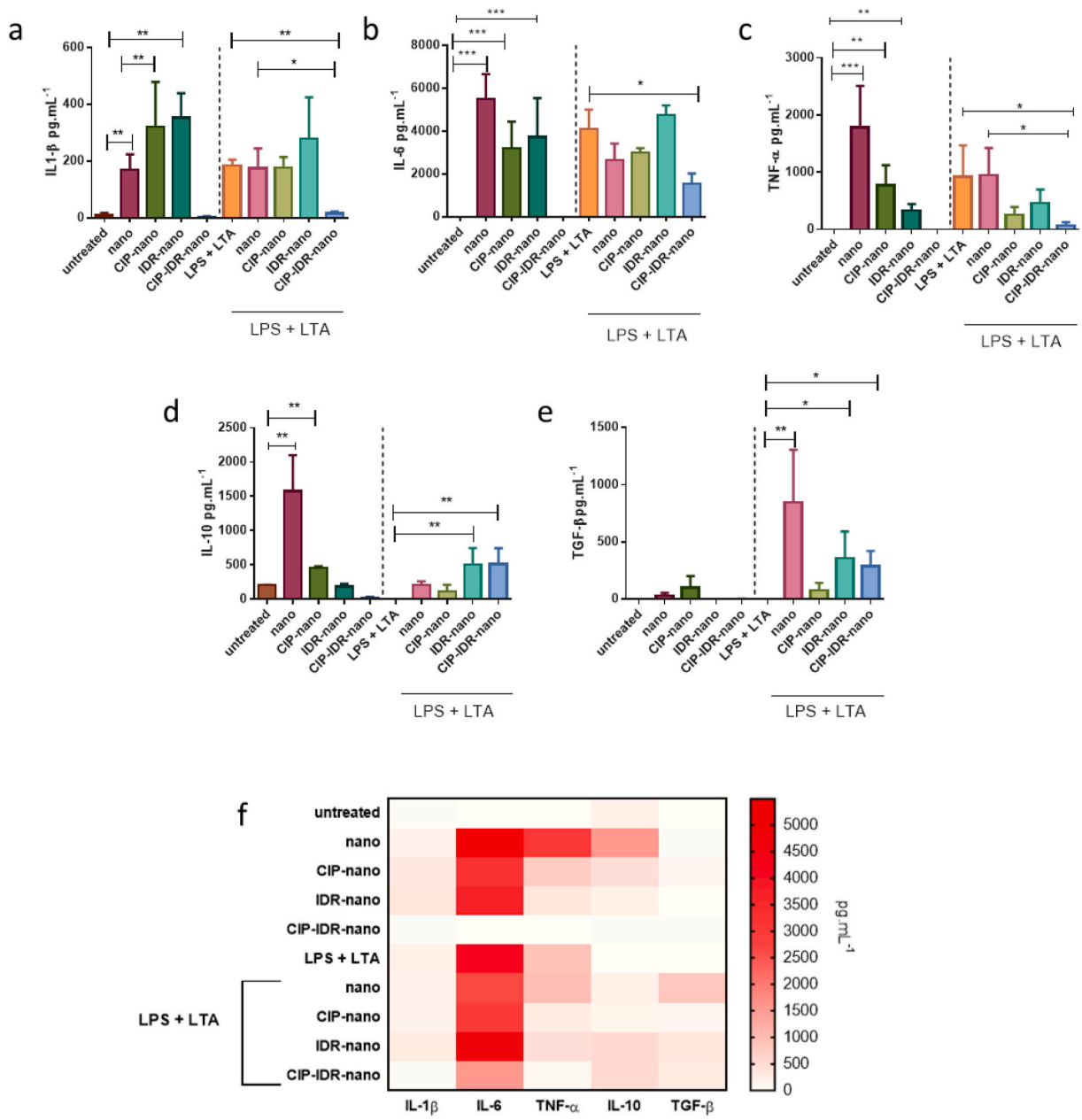

Fig. 6. Immunomodulatory activity of nanofibers. PBMCs were stimulated with nanofiber in the presence or absence of LPS and LTA. IL-1β (a), IL-6 (b), TNF-α (c), IL-10 (d), and TGF-β (e) production was measured after 24 h of incubation by ELISA. Bars represent the average cytokine production in $pg.mL^{-1}$. Statistical differences were represented by * $p < 0.05$, **$p < 0.01$, and ***$p < 0.001$ after one-way ANOVA post Bonferroni test. In (f) the heatmap is a summary of the general immunomodulatory activity of nanofibers (nano), nanofibers with CIP (CIP-nano), IDR-1002 (IDR-nano) or both (CIP-IDR-nano). Red areas illustrate higher cytokine production in $pg.mL^{-1}$.

evaluated with regards their physical contact using SEM. It was observed that SCAPs could adhere on the nanofiber surfaces in control nanofibers (7e-f) and CIP-IDR-nanofibers (Fig. 7g–h). It was observed that cellular extensions of SCAPs embraced nanofibers, creating a favorable complex on which to form new pulp tissue (Fig. 7e–h).

An *in vivo* test was performed after 3 months. Empty fragments and fragments containing only cells were used as controls (Fig. 8a–d). We observed that the presence of a scaffold was critical for tissue formation. Cultures containing only SCAPs did not form connective tissue inside the root fragments (Fig. 8e–h). In contrast, all groups containing control nanofibers, CIP-nanofibers, IDR-nanofibers and CIP-IDR-nanofibers presented a higher new connective tissue formation inside fragments (Fig. 8i-y) ($p < 0.01$) ($p < 0.05$). Control nanofibers stimulated both fibrous and organized tissue and loose connective tissue (Figure 8y). Regarding IDR-nanofibers (Fig. 8q-t) and CIP-IDR-nanofibers (Fig. 8u-x), both stimulated loose connective tissues (Figure 8y). These scaffolds were capable of stimulate the formation of tissue rich in blood vessels. Furthermore, the groups containing nanofibers, especially IDR-1002 presented a lower inflammatory number of cells compared to the empty ($p < 0.01$) and only cells ($p < 0.01$) groups (Fig. 8z), which confirms their promising immunomodulatory potential found *in vitro*. Despite these favorable results found with IDR-1002, there was no evidence regarding the role of this HDP on SCAPs and pulp revascularization/regeneration. This peptide might contribute to the new tissue formation via the immune system [63]. The use of host defense peptides for regenerative endodontics is a promising field that should be explored. Previously the regenerative potential of the host defense peptide LL-37 on SCAPs was tested. This cathelicidin was able to induce

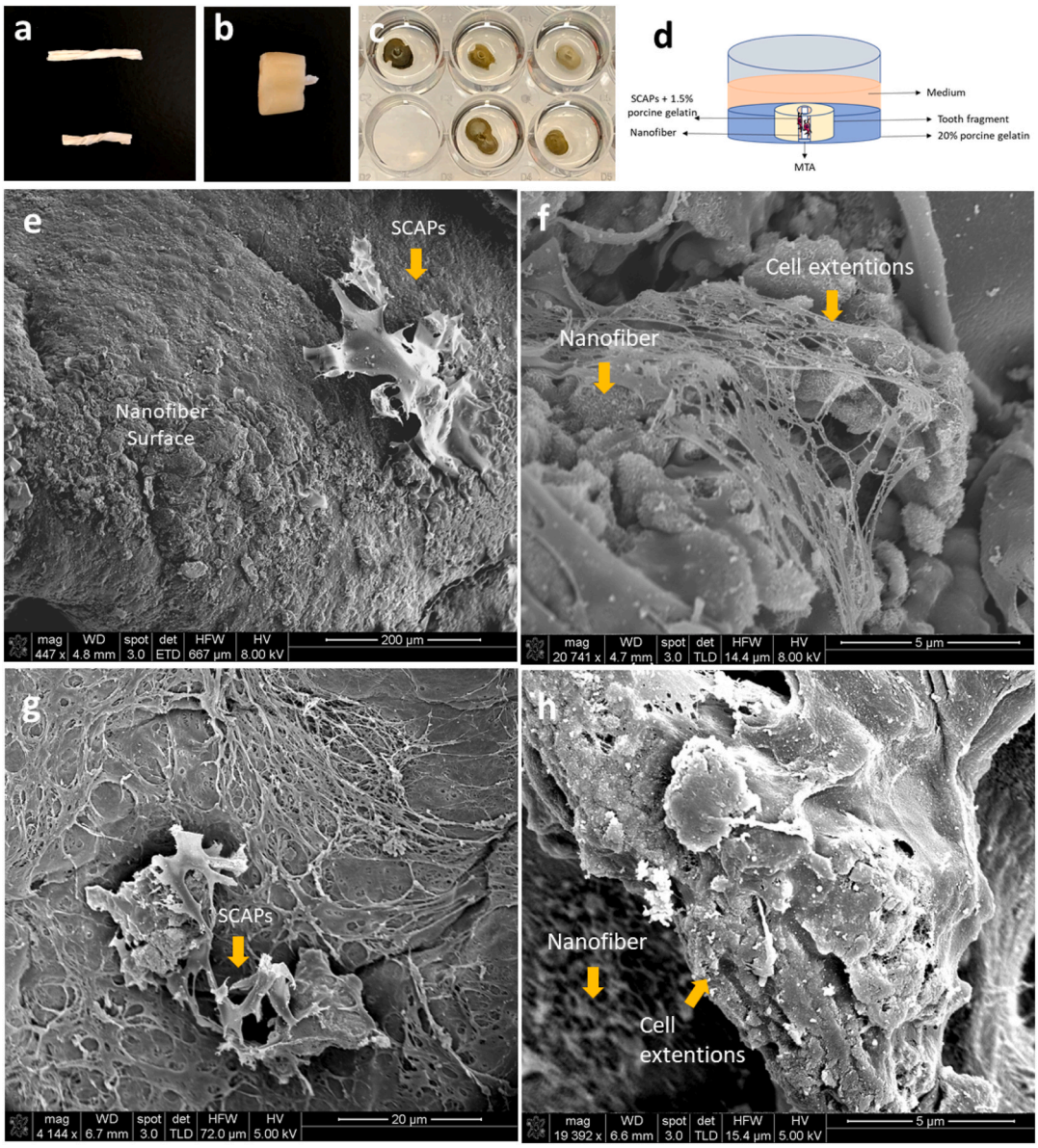

Fig. 7. Nanofiber interaction with SCAPs through SEM. Nanofibers were cut, 3D modeled and cultivated *in vitro* to interact for three days with SCAPs (a–d). These constructs involving SCAPs and nanofibers (e–f), or SCAPs and nanofibers containing ciprofloxacin and IDR-1002 (g–h) are shown with different length (5–200 μm).

cell migration and odonto/osteogenic differentiation of stem cells from the apical papilla likely through the Akt/Wnt/β-catenin signaling pathway [64].

4. Conclusion

In summary, different scaffolds for the endodontic regenerative process were proposed, and nanofibers were chosen as the most suitable scaffold for this process, selecting scaffolds that were degraded over a period of 21 days. Furthermore, we incorporated ciprofloxacin (0.5%) and IDR-1002 (0.5%) into CS/PVA nanofibers. These nanofibers were efficient against *E. faecalis* and *S. aureus* planktonic and biofilms. These scaffolds were also promising against oral biofilms. The developed scaffolds were non-toxic against most of the cells present in the pulp space during the regenerative process. In addition, they did not demonstrate any degree of cytotoxicity against different human cells. As a multifunctional biomaterial, CIP-IDR-nanofibers presented an interesting anti-inflammatory profile. They allowed intense adherence of stem cells from the apical papilla on their surface when cultivated *in vitro* in a 3D cellular model. The *in vivo* data revealed that all nanofibers incorporated with IDR-1002 stimulated a pulp-like tissue inside teeth fragments, and showing very low inflammatory infiltration.

The development of smart anti-biofilm and immunomodulatory nanomaterials is an important advance that links different knowledge areas benefiting human health. Furthermore, these results help to bring HDPs closer to industrial application, designing new platforms for drug-delivery. Thus, this multifunctional prototype of a nanofibrous filling might contribute to the endodontic regenerative process, preserving more dental elements in the oral cavity and boosting oral health quality for endodontic patients.

CRediT authorship contribution statement

Mauricio Gonçalves da Costa Sousa: Conceptualization, Methodology, Validation, Investigation, Data curation, Writing – original draft, Writing – review & editing, Visualization. **Gabriela Conceição de Almeida:** Methodology, Investigation. **Danilo César Martins Mota:** Methodology, Investigation, Visualization. **Rosiane Andrade da Costa:**

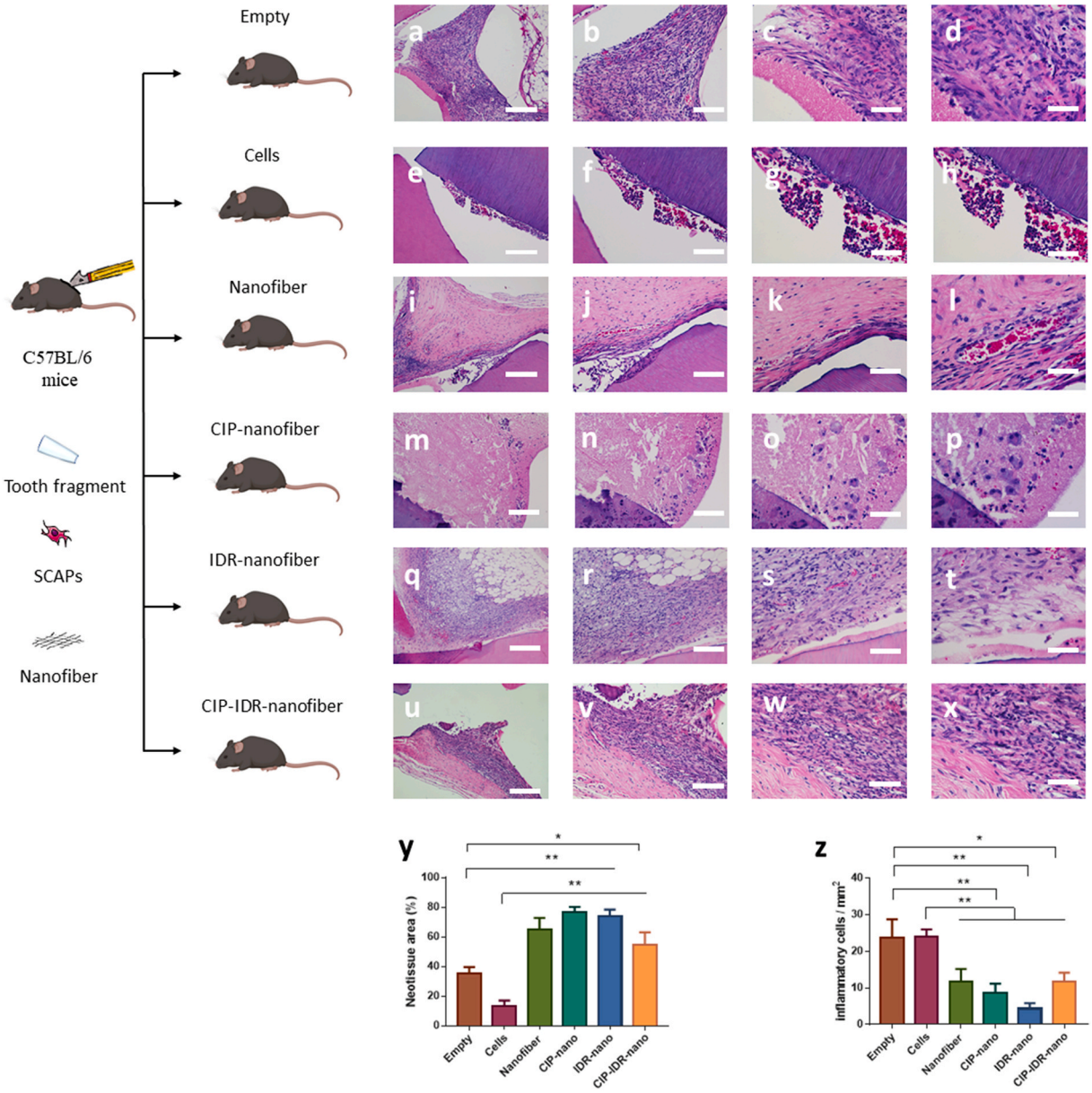

Fig. 8. Hematoxylin and eosin (HE) staining images of the pulp-like tissue formed inside teeth fragments implanted in mice after 3 months. (a–d) represents empty teeth, (e–h) only SCAPs cells, (i–l) nanofibers, (m–p) nanofibers containing ciprofloxacin, (q–t) nanofibers containing IDR-1002, and (u–x) nanofibers containing ciprofloxacin and IDR-1002. Images were processed and organized in four different scales: 10 μm (8a, 8e, 8i, 8 m, 8q, 8u), 20 μm (8b, 8f, 8j, 8n, 8r, 8v), 40 μm (8c, 8g, 8k, 8°, 8s, 8w) and 60 μm (8d, 8h, 8l, 8p, 8t, 8×). 8y represents the percentage of neotissue area formed with the different treatments (empty, cells, nanofibers, CIP-nanofibers, IDR-nanofibers or CIP-IDR-nanofibers). 8z represents the average of inflammatory infiltrate cells after 90 days of treatment with cells, nanofibers, CIP-nanofibers, IDR-nanofibers or CIP-IDR-nanofibers. Statistical differences are represented by * ($p < 0.05$), ** ($p < 0.01$), and *** ($p < 0.001$), after one-way Anova post Bonferroni test.

Conceptualization, Methodology, Validation. **Simoni Campos Dias:** Conceptualization, Methodology. **Samuel Nunes Limberger:** Conceptualization, Methodology. **Frank Ko:** Conceptualization, Methodology, Validation, Supervision, Resources. **Li Ting Lin:** Conceptualization, Methodology, Validation. **Evan F. Haney:** Conceptualization, Methodology, Writing – review & editing. **Hashem Etayash:** Conceptualization, Methodology, Writing – review & editing. **Beverlie Baquir:** Conceptualization, Methodology, Writing – review & editing. **Michael J. Trimble:** Conceptualization, Methodology. **Ya Shen:** Conceptualization, Methodology, Validation, Supervision, Resources. **Zheng Su:** Conceptualization, Methodology. **Markus Haapasalo:** Conceptualization, Methodology, Validation, Supervision, Resources. **Daniel Pletzer:** Conceptualization, Methodology, Writing – review & editing. **Letícia Chaves de Souza:** Conceptualization, Methodology, Writing – review & editing. **Gláucia Schuindt Teixeira:** Methodology, Investigation, Visualization. **Renato M. Silva:** Conceptualization, Methodology, Validation, Supervision, Resources, Writing – review & editing. **Robert E.W. Hancock:** Conceptualization, Methodology, Validation, Supervision, Resources, Writing – review & editing. **Octavio Luiz Franco:** Conceptualization, Methodology, Validation, Supervision, Resources, Writing – review & editing. **Taia Maria Berto Rezende:** Conceptualization, Methodology, Validation, Supervision, Resources, Writing – review & editing, Project administration.

Declaration of competing interest

All authors have contributed to the development of this original research. Furthermore, all authors have read and approved the

manuscript. This article is original and not under publication consideration elsewhere. E.F.H. and R.E.W.H. have invented and filed for patent protection on related antibiofilm peptide sequences. This patent has been assigned to their employer, the University of British Columbia, and has been licensed to ABT Innovations Inc., in which R.E.W.H. has an ownership position. ABT Innovations Inc. is a subsidiary of ASEP Medical Holdings. E.F.H is employed by ASEP and receives salary while R.E.W.H. holds an executive position and is on the Board of ASEP.

Acknowledgments

This study was supported by Conselho Nacional de Desenvolvimento Científico e Tecnológico (CNPq) (409196/2018–5), Coordenação de Aperfeiçoamento de Pessoal de Nível Superior (CAPES) (88887.202222/2018–00), Fundação de Apoio à Pesquisa do Distrito Federal (FAPDF) (00193–00000782/2021-63), and Fundação de Apoio ao Desenvolvimento do Ensino, Ciência e Tecnologia do Estado de Mato Grosso do Sul (FUNDECT) (59/300.397/2015; 022/2018; 028973). In addition, this study was supported by a Canadian Institutes of Health Research Foundation grant FDN-154287 to R.E.W. Hancock. HE is the recipient of a UBC Killam Fellowship and a Research Trainee Award from the Michael Smith Foundation for Health Research (MSFHR). R.E.W. Hancock is a Canada Research Chair in Health and Genomics and a UBC Killam Professor. We also acknowledge Professor Marcelo Oliveira Rodrigues and Chemistry Institute (University of Brasilia) for all support.

Appendix A. Supplementary data

Supplementary data to this article can be found online at https://doi.org/10.1016/j.bioactmat.2022.01.027.

References

[1] B.G. Bishop, G.W. Woollard, Modern endodontic therapy for an incompletely developed tooth, Gen Dent. http://www.ncbi.nlm.nih.gov/pubmed/12116513, 2002, 30, 252-258.
[2] A. Blokland, R.G. Watt, G. Tsakos, A. Heilmann, Traumatic dental injuries and socioeconomic position - findings from the Children's Dental Health Survey 2013, Community Dent. Oral Epidemiol. 44 (2016) 586–591, https://doi.org/10.1111/cdoe.12252.
[3] I.Y. Jung, S.J. Lee, K.M. Hargreaves, Biologically based treatment of immature permanent teeth with pulpal necrosis: a case series, J. Endod. 34 (2008) 876–887, https://doi.org/10.1016/j.joen.2008.03.023.
[4] H. Dhillon, M. Kaushik, R. Sharma, Regenerative endodontics–Creating new horizons, J. Biomed. Mater. Res. B Appl. Biomater. 104 (2016) 676–685, https://doi.org/10.1002/jbm.b.33587.
[5] L.M. Lin, E. Shimizu, J.L. Gibbs, S. Loghin, D. Ricucci, Histologic and histobacteriologic observations of failed revascularization/revitalization therapy: a case report, J. Endod. 40 (2014) 291–295, https://doi.org/10.1016/j.joen.2013.08.024.
[6] S.M.D.F. Lima, M.G.D.C. Sousa, M.D.S. Freire, J.A.D. Almeida, A.P.D.C. Cantuária, T.A.M.E. Silva, C.G.D. Freitas, S.C. Dias, O.L. Franco, T.M.B. Rezende, Immune response profile against persistent endodontic pathogens Candida albicans and Enterococcus faecalis in vitro, J. Endod. 41 (2015), https://doi.org/10.1016/j.joen.2015.02.016.
[7] C. Zhang, J. Du, Z. Peng, Correlation between Enterococcus faecalis and persistent intraradicular infection compared with primary intraradicular infection: a systematic review, J. Endod. 41 (2015) 1207–1213, https://doi.org/10.1016/j.joen.2015.04.008.
[8] B. Kouidhi, K. Fdhila, R. Ben Slama, K. Mahdouani, H. Hentati, F. Najjari, A. Bakhrouf, K. Chaieb, Molecular detection of bacteria associated to dental caries in 4-12-year-old Tunisian children, Microb. Pathog. 71–72 (2014) 32–36, https://doi.org/10.1016/j.micpath.2014.04.008.
[9] D.F. Kinane, P.G. Stathopoulou, P.N. Papapanou, Periodontal diseases, Nat. Rev. Dis. Prim. 3 (2017), https://doi.org/10.1038/nrdp.2017.38.
[10] X. Kuang, V. Chen, X. Xu, Novel approaches to the control of oral microbial biofilms, Biomed Res. Int. 2018 (2018), https://doi.org/10.1155/2018/6498932.
[11] M.M.Y. Khorasani, G. Hassanshahi, A. Brodzikowska, H. Khorramdelazad, Role(s) of cytokines in pulpitis: latest evidence and therapeutic approaches, Cytokine 126 (2020), https://doi.org/10.1016/j.cyto.2019.154896.
[12] S.G. Kim, M. Malek, A. Sigurdsson, L.M. Lin, B. Kahler, Regenerative endodontics: a comprehensive review, Int. Endod. J. 51 (2018) 1367–1388, https://doi.org/10.1111/iej.12954.
[13] J. Yang, G. Yuan, Z. Chen, Pulp regeneration: current approaches and future challenges, Front. Physiol. 7 (2016) 58, https://doi.org/10.3389/fphys.2016.00058.
[14] F. Guerrero, A. Mendoza, D. Ribas, K. Aspiazu, Apexification: a systematic review, J. Conserv. Dent. 21 (2018) 462, https://doi.org/10.4103/JCD.JCD_96_18.
[15] V. Rosa, N. Dubey, I. Islam, K.S. Min, J.E. Nor, Pluripotency of stem cells from human exfoliated deciduous teeth for tissue engineering, Stem Cells Int. 2016 (2016), 5957806, https://doi.org/10.1155/2016/5957806.
[16] S.R. Simon, P.L. Tomson, A. Berdal, Regenerative endodontics: regeneration or repair? J. Endod. 40 (2014) S70–S75, https://doi.org/10.1016/j.joen.2014.01.024.
[17] S.G. Kim, Biological molecules for the regeneration of the pulp-dentin complex, Dent. Clin. 61 (2017) 127–141, https://doi.org/10.1016/j.cden.2016.08.005.
[18] G.T. Huang, F. Garcia-Godoy, Missing concepts in de novo pulp regeneration, J. Dent. Res. 93 (2014) 717–724, https://doi.org/10.1177/0022034514537829.
[19] S. Mai, M.T. Mauger, L.N. Niu, J.B. Barnes, S. Kao, B.E. Bergeron, J.Q. Ling, F. R. Tay, Potential applications of antimicrobial peptides and their mimics in combating caries and pulpal infections, Acta Biomater. (2016), https://doi.org/10.1016/j.actbio.2016.11.026.
[20] S.M.F. Lima, G.M. de Pádua, M.G.C. Sousa, M.S. Freire, O.L. Franco, T.M. B. Rezende, Antimicrobial peptide-based treatment for endodontic infections - biotechnological innovation in endodontics, Biotechnol. Adv. 33 (2015), https://doi.org/10.1016/j.biotechadv.2014.10.013.
[21] R.T. Sousa MGC, P.D. Xavier, A.P.C. Cantuaria, R.A. Porcino, J.A. Almeida, O. L. Franco, Host defense peptide IDR-1002 associated with ciprofloxacin as a new antimicrobial and immunomodulatory strategy for dental pulp revascularization therapy, Microb. Pathog. (2020).
[22] M.T. Albuquerque, M.C. Valera, M. Nakashima, J.E. Nor, M.C. Bottino, Tissue-engineering-based strategies for regenerative endodontics, J. Dent. Res. 93 (2014) 1222–1231, https://doi.org/10.1177/0022034514549809.
[23] M.C. Bottino, K. Kamocki, G.H. Yassen, J.A. Platt, M.M. Vail, Y. Ehrlich, K. J. Spolnik, R.L. Gregory, Bioactive nanofibrous scaffolds for regenerative endodontics, J. Dent. Res. 92 (2013) 963–969, https://doi.org/10.1177/0022034513505770.
[24] S.G. Kim, M. Malek, A. Sigurdsson, L.M. Lin, B. Kahler, Regenerative endodontics: a comprehensive review, Int. Endod. J. (2018), https://doi.org/10.1111/iej.12954.
[25] M.G.C. Sousa, M.R. Maximiano, R.A. Costa, T.M.B. Rezende, O.L. Franco, Nanofibers as drug-delivery systems for infection control in dentistry, Expet Opin. Drug Deliv. (2020) 1–12, https://doi.org/10.1080/17425247.2020.1762564.
[26] K. Balagangadharan, S. Dhivya, N. Selvamurugan, Chitosan based nanofibers in bone tissue engineering, Int. J. Biol. Macromol. 104 (2017) 1372–1382, https://doi.org/10.1016/j.ijbiomac.2016.12.046.
[27] V. Raeisdasteh Hokmabad, S. Davaran, A. Ramazani, R. Salehi, Design and fabrication of porous biodegradable scaffolds: a strategy for tissue engineering, J. Biomater. Sci. Polym. Ed. 28 (2017) 1797–1825, https://doi.org/10.1080/09205063.2017.1354674.
[28] E.A. Kamoun, E.-R.S. Kenawy, X. Chen, A review on polymeric hydrogel membranes for wound dressing applications: PVA-based hydrogel dressings, J. Adv. Res. 8 (2017) 217–233, https://doi.org/10.1016/j.jare.2017.01.005.
[29] M. Mir, M.N. Ali, A. Barakullah, A. Gulzar, M. Arshad, S. Fatima, M. Asad, Synthetic polymeric biomaterials for wound healing: a review, Prog. Biomater. 7 (2018) 1–21, https://doi.org/10.1007/s40204-018-0083-4.
[30] P. Vashisth, N. Raghuwanshi, A.K. Srivastava, H. Singh, H. Nagar, V. Pruthi, Ofloxacin loaded gellan/PVA nanofibers - synthesis, characterization and evaluation of their gastroretentive/mucoadhesive drug delivery potential, Mater. Sci. Eng. C. Mater. Biol. Appl. 71 (2017) 611–619, https://doi.org/10.1016/j.msec.2016.10.051.
[31] J. Jalvandi, M. White, Y. Gao, Y.B. Truong, R. Padhye, I.L. Kyratzis, Polyvinyl alcohol composite nanofibres containing conjugated levofloxacin-chitosan for controlled drug release, Mater. Sci. Eng. C. Mater. Biol. Appl. 73 (2017) 440–446, https://doi.org/10.1016/j.msec.2016.12.112.
[32] K. Chen, J. Liu, X. Yang, D. Zhang, Preparation, optimization and property of PVA-HA/PAA composite hydrogel, Mater. Sci. Eng. C. Mater. Biol. Appl. 78 (2017) 520–529, https://doi.org/10.1016/j.msec.2017.04.117.
[33] T. Alencar-Silva, A. Zonari, D. Foyt, M. Gang, R. Pogue, F. Saldanha-Araujo, S. C. Dias, O.L. Franco, J.L. Carvalho, IDR-1018 induces cell proliferation, migration, and reparative gene expression in 2D culture and 3D human skin equivalents, J. Tissue Eng. Regen. Med. (2019), https://doi.org/10.1002/term.2953.
[34] S.D. Sarkar, B.L. Farrugia, T.R. Dargaville, S. Dhara, Physico-chemical/biological properties of tripolyphosphate cross-linked chitosan based nanofibers, Mater. Sci. Eng. C. Mater. Biol. Appl. 33 (2013) 1446–1454, https://doi.org/10.1016/j.msec.2012.12.066.
[35] D. Pankajakshan, S.L. Voytik-Harbin, J.E. Nör, M.C. Bottino, Injectable highly tunable oligomeric collagen matrices for dental tissue regeneration, ACS Appl. Bio Mater. 3 (2020), https://doi.org/10.1021/acsabm.9b00944.
[36] M.G.C. Sousa, P.D. Xavier, A.P. de C. Cantuária, R.A. Porcino, J.A. Almeida, O. L. Franco, T.M.B. Rezende, Host defense peptide IDR-1002 associated with ciprofloxacin as a new antimicrobial and immunomodulatory strategy for dental pulp revascularization therapy, Microb. Pathog. 152 (2021), https://doi.org/10.1016/J.MICPATH.2020.104634.
[37] D.W. Chen, Y.-H. Hsu, J.-Y. Liao, S.-J. Liu, J.-K. Chen, S.W.-N. Ueng, Sustainable release of vancomycin, gentamicin and lidocaine from novel electrospun sandwich-structured PLGA/collagen nanofibrous membranes, Int. J. Pharm. 430 (2012) 335–341, https://doi.org/10.1016/j.ijpharm.2012.04.010.

[38] T. Zhang, Z. Wang, R.E. Hancock, C. de la Fuente-Nunez, M. Haapasalo, Treatment of oral biofilms by a D-enantiomeric peptide, PLoS One 11 (2016), e0166997, https://doi.org/10.1371/journal.pone.0166997.
[39] E.F. Haney, M.J. Trimble, J.T. Cheng, Q. Vallé, R.E.W. Hancock, Critical assessment of methods to quantify biofilm growth and evaluate antibiofilm activity of host defence peptides, Biomolecules 8 (2018), https://doi.org/10.3390/biom8020029.
[40] D. Wang, M. Haapasalo, Y. Gao, J. Ma, Y. Shen, Antibiofilm peptides against biofilms on titanium and hydroxyapatite surfaces, Bioact. Mater. 3 (2018) 418–425, https://doi.org/10.1016/j.bioactmat.2018.06.002.
[41] ISO E, 10993-5, Biological Evaluation of Medical Devices. Part 5: Tests for in Vitro Cytotoxicity - Pesquisa Google, International Organization for Standardization, Geneva, Switzerland, 2009.
[42] T. Mosmann, Rapid colorimetric assay for cellular growth and survival: application to proliferation and cytotoxicity assays, J Immunol Methods. http://www.ncbi.nlm.nih.gov/pubmed/6606682, 1983, 65, 55-63.
[43] G. Fotakis, J.A. Timbrell, In vitro cytotoxicity assays: comparison of LDH, neutral red, MTT and protein assay in hepatoma cell lines following exposure to cadmium chloride, Toxicol. Lett. 160 (2006) 171–177, https://doi.org/10.1016/j.toxlet.2005.07.001.
[44] M. Yadlapati, C. Biguetti, F. Cavalla, F. Nieves, C. Bessey, P. Bohluli, G.P. Garlet, A. Letra, W.D. Fakhouri, R.M. Silva, Characterization of a vascular endothelial growth factor-loaded bioresorbable delivery system for pulp regeneration, J. Endod. 43 (2017) 77–83, https://doi.org/10.1016/j.joen.2016.09.022.
[45] B.H.A. Mai, M. Drancourt, G. Aboudharam, Ancient dental pulp: masterpiece tissue for paleomicrobiology, Mol. Genet. Genomic Med. 8 (2020), https://doi.org/10.1002/mgg3.1202.
[46] D. Lukic, L. Karygianni, M. Flury, T. Attin, T. Thurnheer, Endodontic-like oral biofilms as models for multispecies interactions in endodontic diseases, Microorganisms 8 (2020), https://doi.org/10.3390/microorganisms8050674.
[47] A.C. Bean, R.S. Tuan, Fiber diameter and seeding density influence chondrogenic differentiation of mesenchymal stem cells seeded on electrospun poly (ε-caprolactone) scaffolds, Biomed. Mater. 10 (2015), https://doi.org/10.1088/1748-6041/10/1/015018.
[48] V.R. Giri Dev, T. Hemamalini, Porous electrospun starch rich polycaprolactone blend nanofibers for severe hemorrhage, Int. J. Biol. Macromol. 118 (2018) 1276–1283, https://doi.org/10.1016/j.ijbiomac.2018.06.163.
[49] S.N. Kaushik, B. Kim, A.M. Walma, S.C. Choi, H. Wu, J.J. Mao, H.W. Jun, K. Cheon, Biomimetic microenvironments for regenerative endodontics, Biomater. Res. 20 (2016) 14, https://doi.org/10.1186/s40824-016-0061-7.
[50] D. Kim, S.-H. Park, Effects of age, sex, and blood pressure on the blood flow velocity in dental pulp measured by Doppler ultrasound technique, Microcirculation 23 (2016) 523–529, https://doi.org/10.1111/micc.12302.
[51] G. Schmalz, M. Widbiller, K.M. Galler, Clinical perspectives of pulp regeneration, J. Endod. 46 (2020) S161–S174, https://doi.org/10.1016/j.joen.2020.06.037.
[52] M.E.E. Wright, A.T. Wong, D. Levitt, I.C. Parrag, M. Yang, J.P. Santerre, Influence of ciprofloxacin-based additives on the hydrolysis of nanofiber polyurethane membranes, J. Biomed. Mater. Res. 106 (2018) 1211–1222, https://doi.org/10.1002/jbm.a.36318.
[53] A.M. Piras, S. Sandreschi, G. Maisetta, S. Esin, G. Batoni, F. Chiellini, Chitosan nanoparticles for the linear release of model cationic peptide, Pharm. Res. (N. Y.) 32 (2015) 2259–2265, https://doi.org/10.1007/s11095-014-1615-9.
[54] P. Verma, A. Nosrat, J.R. Kim, J.B. Price, P. Wang, E. Bair, H.H. Xu, A.F. Fouad, Effect of residual bacteria on the outcome of pulp regeneration in vivo, J. Dent. Res. 96 (2017) 100–106, https://doi.org/10.1177/0022034516671499.
[55] E. Brambilla, A. Ionescu, A. Mazzoni, M. Cadenaro, M. Gagliani, M. Ferraroni, F. Tay, D. Pashley, L. Breschi, Hydrophilicity of dentin bonding systems influences in vitro Streptococcus mutans biofilm formation, Dent. Mater. 30 (2014) 926–935, https://doi.org/10.1016/j.dental.2014.05.009.
[56] J.L. Baker, B. Bor, M. Agnello, W. Shi, X. He, Ecology of the oral microbiome: beyond bacteria, Trends Microbiol. 25 (2017) 362–374, https://doi.org/10.1016/j.tim.2016.12.012.
[57] L.S. Gu, X. Cai, J.M. Guo, D.H. Pashley, L. Breschi, H.H.K. Xu, X.Y. Wang, F.R. Tay, L.N. Niu, Chitosan-based extrafibrillar demineralization for dentin bonding, J. Dent. Res. 98 (2019) 186–193, https://doi.org/10.1177/0022034518805419.
[58] A.F. Fouad, Contemporary microbial and antimicrobial considerations in regenerative endodontic therapy, J. Endod. 46 (2020) S105–S114, https://doi.org/10.1016/j.joen.2020.06.030.
[59] C. Stambolsky, S. Rodríguez-Benítez, J.L. Gutiérrez-Pérez, D. Torres-Lagares, J. Martín-González, J.J. Segura-Egea, Histologic characterization of regenerated tissues after pulp revascularization of immature dog teeth with apical periodontitis using tri-antibiotic paste and platelet-rich plasma, Arch. Oral Biol. 71 (2016) 122–128, https://doi.org/10.1016/j.archoralbio.2016.07.007.
[60] L. Chung, D.R. Maestas, F. Housseau, J.H. Elisseeff, Key players in the immune response to biomaterial scaffolds for regenerative medicine, Adv. Drug Deliv. Rev. 114 (2017) 184–192, https://doi.org/10.1016/j.addr.2017.07.006.
[61] H.B.T. Moran, J.L. Turley, M. Andersson, E.C. Lavelle, Immunomodulatory properties of chitosan polymers, Biomaterials 184 (2018) 1–9, https://doi.org/10.1016/j.biomaterials.2018.08.054.
[62] C. Hadjichristou, I. About, P. Koidis, A. Bakopoulou, Advanced in vitro experimental models for tissue engineering-based reconstruction of a 3D dentin/pulp complex: a literature review, Stem Cell Rev. Rep. (2020), https://doi.org/10.1007/s12015-020-10069-8.
[63] A. Huante-Mendoza, O. Silva-García, J. Oviedo-Boyso, R.E.W. Hancock, V. M. Baizabal-Aguirre, Peptide IDR-1002 inhibits NF-κB nuclear translocation by inhibition of IκBα degradation and activates p38/ERK1/2-MSK1-dependent CREB phosphorylation in macrophages stimulated with lipopolysaccharide, Front. Immunol. 7 (2016), https://doi.org/10.3389/FIMMU.2016.00533.
[64] Q. Cheng, K. Zeng, Q. Kang, W. Qian, W. Zhang, Q. Gan, W. Xia, The antimicrobial peptide LL-37 promotes migration and odonto/osteogenic differentiation of stem cells from the apical papilla through the akt/wnt/β-catenin signaling pathway, J. Endod. 46 (2020) 964–972, https://doi.org/10.1016/j.joen.2020.03.013.